Surface & Coatings Technology 362 (2019) 388–396

Contents lists available at ScienceDirect

Surface & Coatings Technology

journal homepage: www.elsevier.com/locate/surfcoat

Fine-tuning of chemical and physical polymer surface modifications by atmospheric pressure post-discharge plasma and its correlation with adhesion improvement

Lucie Brès[a,b], Audrey Sanchot[a,b], Bertrand Rives[a], Nicolas Gherardi[b], Nicolas Naudé[b,*], Maëlenn Aufray[c]

[a] IRT Saint-Exupéry, Toulouse, France
[b] LAPLACE, Université de Toulouse, CNRS, Toulouse, France
[c] CIRIMAT, Université de Toulouse, CNRS, INPT, UPS, 4 allée Émile Monso, BP 44362, 31030 Toulouse, France

ARTICLE INFO

Keywords:
Three-point bending test
Cross-cut test
Adhesion mechanisms
Atmospheric pressure plasma
PEEK matrix

ABSTRACT

Our study focuses on the use of a remote atmospheric pressure plasma process for the improvement of polymer surface reactivity. Indeed, surface activation of carbon-fiber-reinforced polymers that use a polyetheretherketone matrix is required to achieve strong and long-term adhesion of paint on the composite. Emphasis will be placed on the contribution of gas plasma used on surface modification. We use two techniques to characterize adherence improvement: a qualitative and industrial approach with a cross-cut test and a quantitative approach with a three-point bending test. However, to provide a better understanding of the plasma-induced modifications using air or nitrogen gas, diagnostics of the surface are also necessary. The wettability improvement, chemical surface modifications, and topography are analyzed by using contact angle measurement, X-ray photoelectron spectroscopy, and atomic force microscopy, respectively. The combination of these diagnostics highlights the capability of plasma treatment to tune the plasma/surface interactions depending on gas plasma, which results in improved adhesion.

1. Introduction

The increasingly widespread use of carbon-fiber-reinforced polymers (CFRPs) in structural engineering can be explained by their low weight coupled with their good mechanical properties [1,2]. Polyetheretherketone (PEEK) matrix composites are particularly appreciated in aeronautic applications because of their high thermal stability and chemical resistance, in conjunction with a good ability to withstand high mechanical loads [3]. The literature shows several studies aimed at improving the surface energy of such materials to obtain strong and durable adhesive properties [4,5]. In this context, knowledge of adhesion mechanisms is fundamental for the control of the PEEK CFRP/coating interface and interphase. This is especially true because these interactions depend on the surface quality and bonding conditions [6].

Nowadays, in industry, surface preparation methods by chemical or mechanical means mostly to combine manual sanding and degreasing. The performance of the implemented method, that is the sanding (with Scotch Brite hand pads), is very operator-dependent because it is a manual process. Moreover, it generates a lot of dust, which can potentially cause contamination and bad adhesion if it is captured under the painting film. Increasingly strict environmental standards and security constraints have led to the development of new technologies for “greener” surface preparation [7]. Atmospheric pressure plasma (APP) processes are particularly promising in this context. From an industrial point of view, one of the strengths of APP for surface preparation, in comparison with mechanical means, is the absence of dust and degradation on a large scale. Furthermore, the process can be partially or fully automated, which introduces robustness and reliability.

Surface activation with APP processes generally consists of modifying the surface free energy or surface reactivity through surface oxidation and chemical grafting [8,9]. Studies have also shown the influence of roughness on the coating wettability after plasma activation. These two complementary effects can lead to an increase in adhesion phenomena at the interface between the coating and composite [10,11]. Some processes involving air or nitrogen gas have been shown to be effective ways to improve the adhesion properties with a coating (paint, glue, or resin) [12,13].

* Corresponding author.
E-mail address: nicolas.naude@laplace.univ-tlse.fr (N. Naudé).

https://doi.org/10.1016/j.surfcoat.2019.01.102
Received 5 July 2018; Received in revised form 25 January 2019; Accepted 28 January 2019
Available online 29 January 2019
0257-8972/ © 2019 Elsevier B.V. All rights reserved.

In this study, we have characterized industrial PEEK composites prior to and after activation with a remote atmospheric pressure cold plasma torch [14]. Two different gas carriers, air and nitrogen, were used to generate the plasma. In addition to adherence tests by cross-cutting and three-point bending, the surface modifications were also investigated by using contact angle measurements, X-ray photoelectron spectroscopy (XPS), and atomic force microscopy (AFM).

2. Materials and methods

2.1. Atmospheric pressure plasma setup

The experimental setup consists of an industrial UL-SCAN arc plasma torch supplied by AcXys Technologies©, which is operated at atmospheric pressure. The discharge is obtained by the breakdown of the gas flowing between two electrodes. An afterglow region over a few centimeters, namely the post-discharge, as indicated Fig. 1, is created at the outlet of the nozzle, which is directed toward the sample [15]. The post-discharge contains reactive species such as metastables, neutrals, and radicals, but not ionized species [9,16].

The working gas can be either dry (dew point temperature $< 3\,^{\circ}C$), oil-free (oil residues $< 0.01\,mg/m^3$), and compressed filtered air (free of particles with diameter $> 0.1\,\mu m$) or compressed nitrogen (99.9998% purity, Air Liquide©). A certain number of process parameters illustrated in Fig. 1 can be tuned by the operator:

- Scan speed of the torch (set at 0.3 m/s);
- Gap which is defined as the distance between the plasma equipment and the substrate (set at 27 mm);
- Gas flow rate ranges from 30 to 60 slm.

2.2. Description of sample

Activations with the remote APP system described above are done on an industrial CFRP with a PEEK matrix. This composite material is manufactured in an autoclave with several carbon plies encapsulated between two glass plies. Hence, the top surface is mainly composed of the PEEK matrix. The composite material shows a visually planar surface, that is slightly rough ($R_a = 3.7 \pm 1.2\,nm$) and is around $2 \times 10^{-3}\,m$ thick. To obtain reproducible initial surfaces before characterization or activation, samples are manually cleaned three times with moistened wipes of propylene glycol methyl ether (Diestone DLS wipes from SOCOMORE©). In this study, an external polyurethane-based coating is applied to untreated and treated PEEK CFRPs. This coating is an industrial paint supplied by Mapaero© that is commonly used on helicopters for protective and aesthetic purposes.

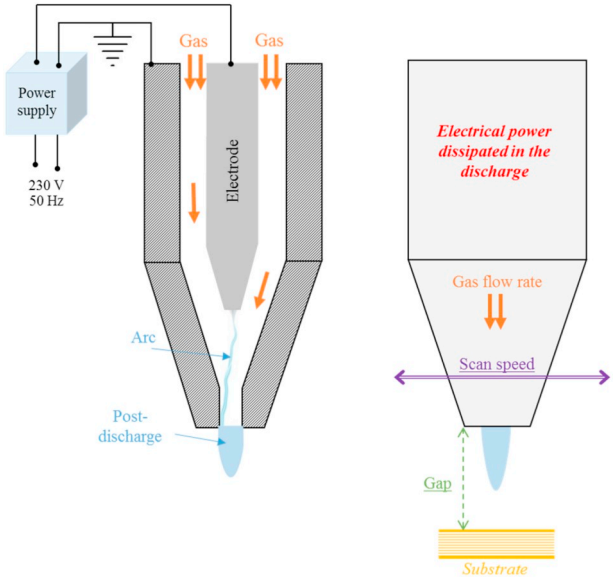


Fig. 1. Schematic representation of the experimental UL-SCAN device.

Table 1
Wettability characteristics of liquids used for contact angle measurements [18]. All data are expressed in mJ/m^2.

Liquid	γ_L	γ_L^D	γ_L^P
Water	72.8	21.8	51
Diiodomethane	50.8	50.8	0

2.3. Wettability measurements

The surface wettability studies by contact angle measurements are carried out by analyzing static sessile drops. A portable dosing instrument called a Mobile Surface Analyzer, developed by KRUSS© is used.

The polarity of the surface is investigated by using the Owens–Wendt–Rabel–Kaelble (OWRK) theory [17]. The Surface Free Energy (SFE) is expressed by Eq. (1), in which γ_S^D and γ_S^P are the dispersive and the polar components of the surface tension, respectively. θ_a represents the contact angle of the probing liquid, and the subscripts L and S, the liquid and solid phases.

$$\gamma_L(1 + cos\,\theta_a) = 2\sqrt{\gamma_S^D \gamma_L^D} + 2\sqrt{\gamma_S^P \gamma_L^P} \quad (1)$$

The characteristics of the two reference liquids for the determination of the SFE components are presented in Table 1. For each sample, repeatability is checked by analyzing three drops of each liquid at room temperature, 5 s after the deposition of the drop.

2.4. Chemical analysis

Surface chemical analysis limited to 5 nm depth is performed with a Kratos® Nova X-ray photoelectron spectrometer by using a monochromatic Al Kα source. The angle measurement of the analysis is settled at a grazing angle of $\theta = 75^{\circ}$ (θ is the angle between the source and the photoelectron detector). An area of $1200\,\mu m \times 700\,\mu m$ is irradiated at the center of the sample. The characterization is performed under a vacuum of approximately 10^{-9} Torr. The binding energies of spectra are corrected by using the C═C bond of the C1s peak at 284.7 eV. The standard deviation of the concentration is 0.1%.

2.5. Topographical analysis

The nanoroughness is characterized with a multimode Nanoscope V microscope (AFM) from Bruker©. Peak Force mode using TESPA probes is selected to scan the surfaces of the composites. The instrument software allows analysis of the topographical images and extraction of two representative parameters from the image: the nanoroughness R_a and the specific surface area S_{dr}. The former represents the arithmetical mean roughness of the analyzed surface. The latter corresponds to the developed interfacial area ratio. This parameter is expressed as a percentage of the additional surface area induced by the texture relative to the planar definition area. The R_a and S_{dr} values are calculated from an average of three $5\,\mu m \times 5\,\mu m$ images on three different samples.

2.6. Interface characterization by three-point bending test

2.6.1. Relevance of the test

Among the wide variety of mechanical tests, three-point bending test according to ISO 14679:1997 [19] presents some advantages in the context of this study. The good repeatability of the results, as a result of the tensile machine, coupled with the numerous types of exploitable information that can be obtained, makes this test useful for a better

understanding of adhesion phenomena [20]. In this latter reference precisely, Genty et al. highlighted the contribution of the three point bending test as a differentiation means for the adhesion characterization. Indeed, this technique has the capacity to get more accurate results compared to an efficient but limited semi-quantitative adhesion test (see paragraph 2.7). Specific samples are dimensioned and manufactured according to the standard for the compliance to the three point bending test. They consist of a PEEK composite coated with an industrial polyurethane paint. A cube of an Araldite® epoxy is formed on the paint for the sole purpose of creating a discontinuity in the strains and focusing the failure initiation on one of the small edges of the stiffener. Application of the epoxy is carried out with a 0.5 mL syringe and the curing cycle of the product is 3 h at room temperature followed by 3 h at 60 ± 5 °C. Obviously, the adherence of the epoxy on the coating has to be higher than that of the PEEK CFRP/coating and it is not measured in this study. A tensile strength is applied on the top of the substrate and the response in force is measured. Force/displacement curves are recorded by the equipment software.

2.6.2. Information and results

Qualitative data is obtained through visual inspection of the failure face and the location of the failure itself. Two types of failure are possible: a cohesive one, which is located within one of the parts of the system, and an adhesive one, which is located at the PEEK CFRP/coating interface [6]. The former reflects the cohesion of the concerned parts, whereas the latter reflects the adherence at the join. Hence, only the maximal load that leads to adhesive failure can help in comparing adherence values among different configurations.

Moreover, quantitative data can be extracted from the load/displacement curve (see Fig. 2):

1) The slope of the linear part of the curve. Corresponds to the mechanical response of the entire system (sample with epoxy cube). Stands for the rigidity of the system and, hence, the repeatability of sample fabrication.
2) The drop-in load. Indicates the adherence failure.
3) The F_{max} value, the ultimate load before failure initiation. Considered as an adherence measurement for the coating on the PEEK substrate. We consider that the ultimate load when an adhesive failure occurs should be higher than the F_{max} value measured for a cohesive failure. In this way, the reported ultimate loads in this study are either equal to (adhesive failure) or lower than or equal to (cohesive failure) the adherence.

2.6.3. Experimental data

Adhesion performance is evaluated by using an INSTRON tensile machine (model 3367) equipped with a three-point bending system and a 5000 N load sensor (error margin of 0.1%). The distance between supporting pins is 35 mm and the speed of test is 0.5 mm/min. The standard prescribes a distance of 33 mm; however, the machine used has a large bending radius that makes it impossible to carry out tests with this distance. The maximum tensile strength value of each interface (recorded with BLUEHILL software) is calculated from the average of eight specimens.

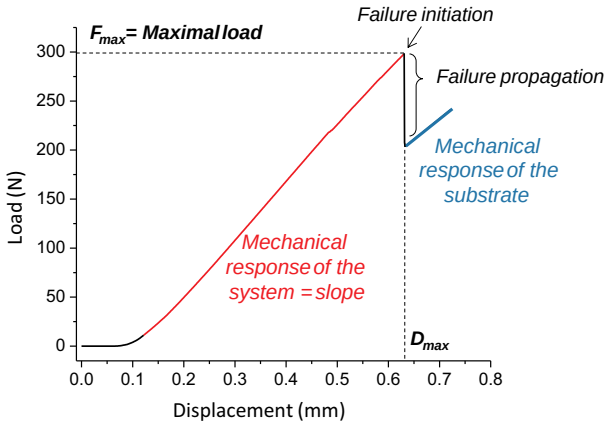


Fig. 2. Information extracted from a load versus displacement curve after a three-point bending test.

2.7. Interface characterization by cross-cut test

Adhesion performances are also evaluated in the widespread industrial way and in accordance with the ISO 2409:2013 standard [21] by using a semi-automated 430 PI cross-cut tester, developed by Erichsen©. Different setting parameters allow good repeatability of the experiments. Among them the force (between 6 and 17 N), the speed (1000 mm/min), the number of cuts (6), and the space between them (spaced by 1 mm). The detailed stages of the standardized test can be found in [21].

A visual inspection of the surface state after tape removal and comparison to a "GT table" of results (from the standard) allows us to classify the adhesion of the substrate: from grade 0 (excellent adhesion) to grade 5 (very bad adhesion). For industry specifications, only GT0 and GT1 are accepted.

2.8. Ageing of panels

During water ageing, painted samples are completely immersed in water, in accordance with the ISO 2812-2:2007 standard [22]. A temperature of 40 ± 1 °C is sustained by using a Memmert™ V76 climatic chamber. In order to meet the specifications of the aeronautical industries, the water ageing test lasts for seven days. Samples are then dried and stored for 24 h before interface characterization.

3. Results and discussion

3.1. Adhesion according to gas plasma

Fig. 3 shows the adherence grades, according to the appendix of the ISO 2409:2013 standard, for non-aged (white areas) and aged (hatched areas) systems as a function of the gas plasma used and the discharge power. Untreated CFRP composites present very bad adherence with the coating, as indicated by the GT5 grade under all conditions. This is in accordance with the fact that the PEEK matrix is usually considered to be quite inert toward coatings [23].

After plasma activation and without the ageing step, the adherence is substantially improved as a grade of GT0 or GT1 is always obtained. Plasma activation improves surface reactivity and, hence, adhesion phenomena. However, no clear distinction is observed in correlation with the gas plasma used or the discharge power. No more precise findings can be made from these initial results. Therefore, we decided to carry out water ageing for seven days to discriminate between the different activation systems.

Hatched bars on the Fig. 3 clearly show different behaviors between the air (a) and nitrogen (b) treatments after water ageing. In the former case, the adherence decreases and it becomes even worse as the power is increased, until it reaches the GT5 grade, which is similar to that for an untreated substrate. In the latter case, an excellent adherence grade is maintained, which suggests different and more efficient activation mechanisms under nitrogen plasma than under air plasma.

To obtain some additional data in order to understand the interface phenomena, a more specific approach is used: the three-point bending test. Reader can refer to the section 2.6 for technical data.

Fig. 4(a) presents the different types of failure obtained after activation, adhesive or cohesive one, in comparison with an untreated and uncovered substrate. Fig. 4(b) and (c) focused on the initiation location, which is always on one of the small edges of the stiffener, as

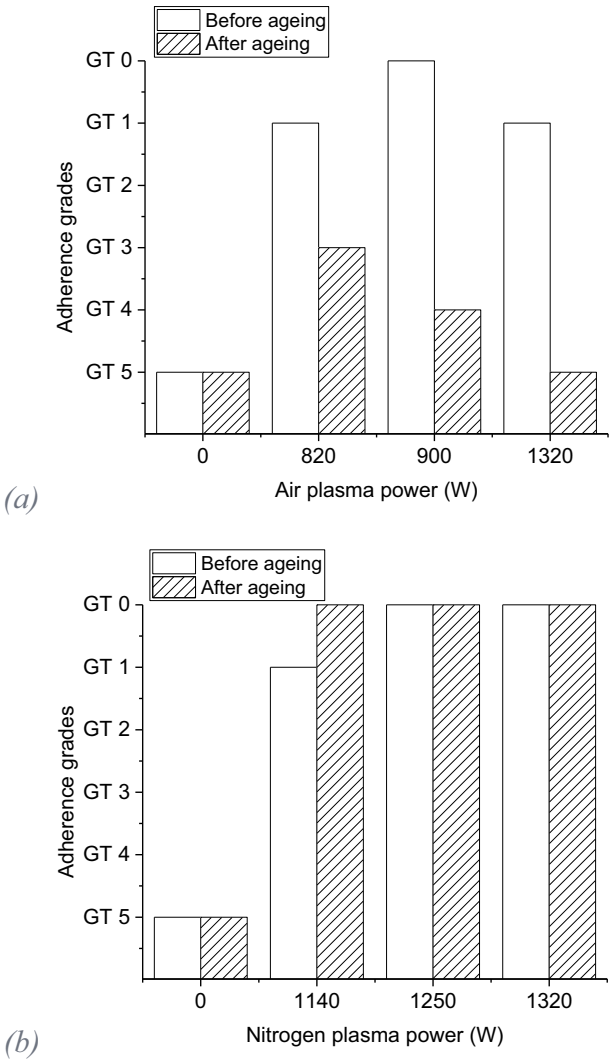


Fig. 3. Adherence grades obtained from cross-cut tests prior to and after water ageing of untreated substrates and substrates activated under (a) air and (b) nitrogen plasmas.

represented by the small arrows in Fig. 4(a). These profiles are achieved after water ageing. Air plasma treated substrates give rise to visual adhesive failure initiation between the PEEK substrate and the coating. After nitrogen plasma treatment, the failure initiation types are both adhesive (between the PEEK substrate and the coating) and cohesive (inside the PEEK matrix). Nevertheless, a larger proportion of adhesive ones is noted.

Fig. 5 presents the evolution of the F_{max} values obtained with a water-aged system after the three-point bending test. It underlines two trends in adherence depending on the plasma gas used. First, under air plasma, a decrease in the value is noted, which is in accordance with the GT grades obtained from the cross-cut test (see Fig. 3). At high discharge power, the F_{max} values are close to that obtained without activation. Unlike the air plasma, nitrogen plasma treatment gives rise to better adherence properties with values that are approximately twice as high as that of the untreated substrate. This is also in good agreement with the cross-cut test results obtained after ageing by immersion in water. We note that the measurement uncertainties are of the same order as those seen in the literature [24].

During the seven days of ageing, water molecules, with their small size, can act as plasticizers in the system, which results in a diminution of the mechanical cohesion of the studied system [25]. More precisely, this phenomenon could appear at different locations:

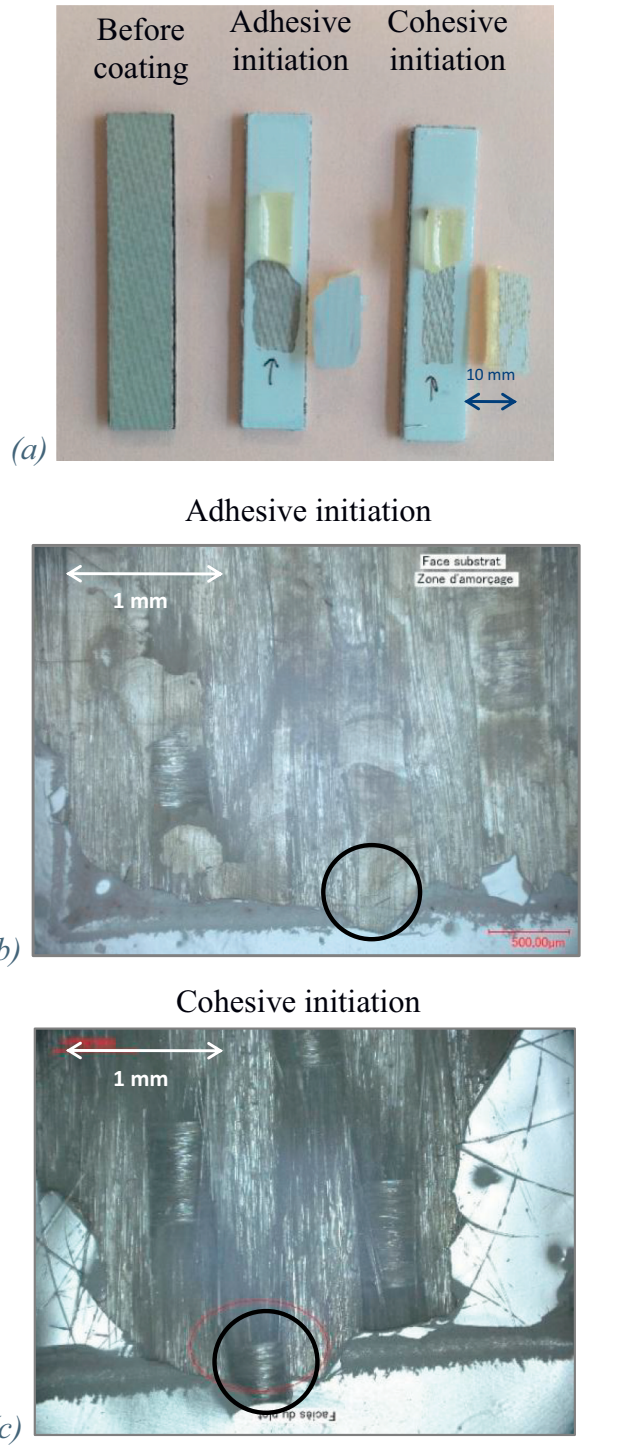


Fig. 4. (a) Fracture surfaces of treated substrates after the three-point bending test showing the two types of initiation, (a) adhesive and (b) cohesive. The location of the initiation is represented by the circles.

- In the PEEK polymer matrix;
- In the coating;
- In the stiffener;
- At the interface between the composite substrate and the coating; or
- At the interface between the coating and the stiffener.

The two distinct trends in the maximal load according to the gas probably originate from different degrees of surface modification during the plasma treatments. One point to check is that the water

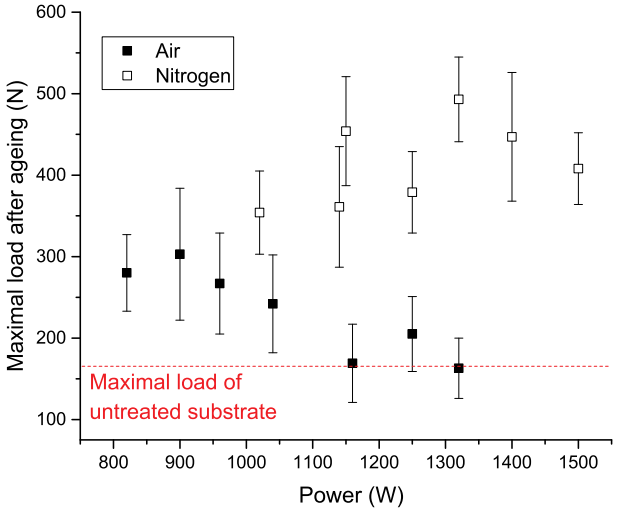


Fig. 5. Maximal load after ageing, relative to power, in the case of air ■ or nitrogen □ plasma treatments. The value before plasma activation is represented on the figure by the dotted line.

ageing done on our final system (the activated and coated PEEK CFRP with the epoxy stiffener) does not influence the measured F_{max} values. Let us not that there is no plasticization of the substrate nor the cube of an Araldite The global properties of the system (rigidity) are maintained and the configurations tested are reproducible. This also confirms that we are correctly measuring the adherence of our PEEK CFRP/coating systems, in cases of both adhesive and cohesive (minimal adherence) failures.

As highlighted in Fig. 5, the maximal load before failure increases after nitrogen plasma treatment up to a power value of about 1300 W, whereas the F_{max} value decreases after treatment with air plasma; this suggests that the surface modification and, hence, the quality of adherence are directly linked to the plasma gas used. At this point, some assumptions can be made with regard to: 1) potential top-surface degradation under air plasma, which is not a long-range mechanism; and 2) the better adherence observed with nitrogen plasma treatment. In this latter case, it seems that saturation is reached after 1300 W and no more improvement could be obtained.

In order to confirm these two hypotheses and gain further understanding, surface characterizations before the mechanical failure are necessary. Indeed, several studies show the relevance of certain theories in explaining the adhesion between a substrate and a polymer coating [26].

From knowledge of the surface interactions, it is possible to identify and predict adhesion mechanisms between two materials. In the next section, we discuss the hydrophilicity and chemical property enhancement of the substrate in the context of the wetting [27] and chemical [28] theories, respectively. The surface morphology modifications will then be considered in section 3.3 with regard to the mechanical anchoring theory [29].

3.2. Study of the wettability and chemical modifications introduced by plasma activation

The wetting and chemical theories describe adhesion mechanisms through intermolecular (such as Van der Waals interactions) and interatomic (covalent or ionic) bonds, respectively [27,28].

Fig. 6(a) shows a decrease in the Water Contact Angle (WCA, θ_w) after both air and nitrogen treatments, with minimal values of around 10° with air plasma and 25° with nitrogen plasma. Nevertheless, the results with air plasma show a variation in θ_{water} according to the power used; this is not visible with nitrogen plasma. From the WCA values, decomposition of the surface free energy is done by using the

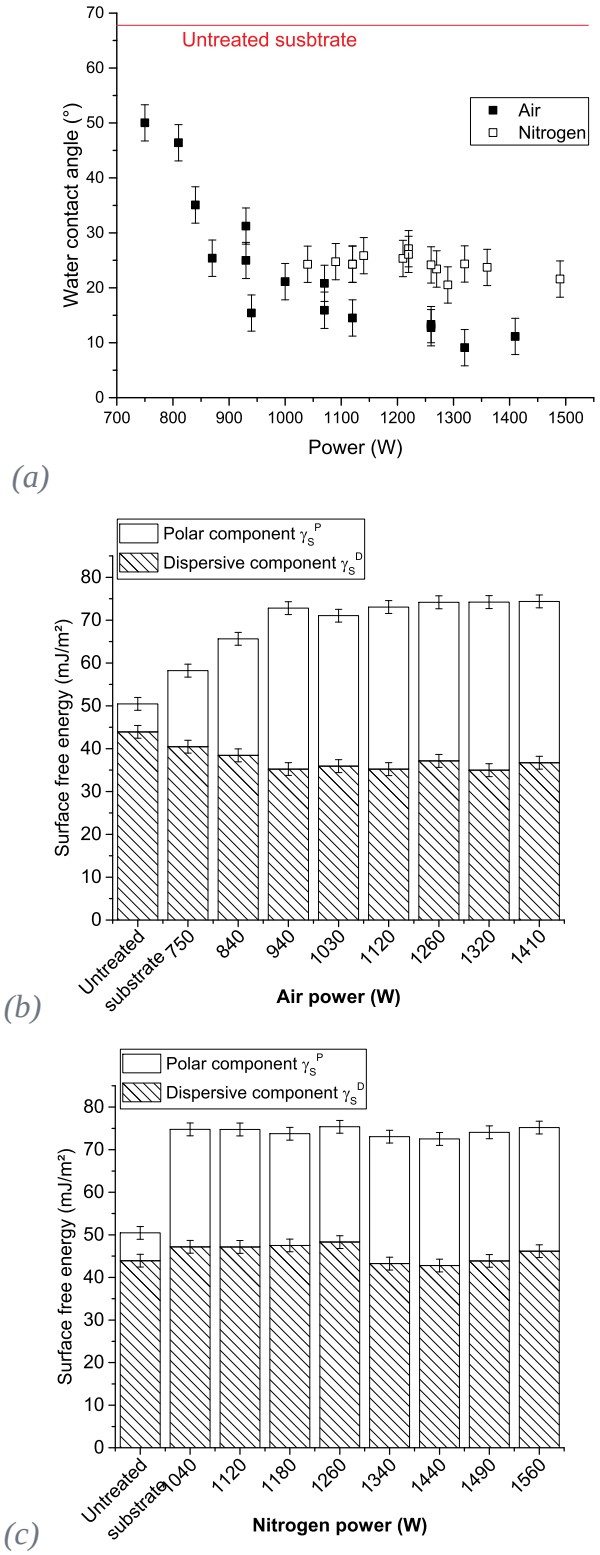


Fig. 6. (a) Water contact angles and surface free energies after (b) air or (c) nitrogen treatment relative to the plasma power.

OWRK model. Fig. 6(b) and (c) reveal the increase in the polar component after plasma treatment. All of the observations indicate an increase in polar groups brought about by plasma activation. However, no significant variation is seen for the dispersive component, which reflects the Van der Waals bonds. This behavior is also described in the literature [30].

Table 2
Chemical composition of untreated and treated substrates relative to plasma power. The results indicate greater surface oxidation with air plasma. Measurements are done with a grazing angle of 75°.

	O/C ratio	% N	Grafting ratio from C1s peak[a]
Untreated substrate	0.16	0.3	0
Air plasma			
820 W	0.35	1	21.7
960 W	0.4	1	28.5
1320 W	0.46	1	31.7
Nitrogen plasma			
1150 W	0.28	1.3	14.7
1250 W	0.32	1.6	16.8
1320 W	0.31	1.3	16.1

[a] Sum of the four contribution concentrations related to grafting: C—O (C—N), C═O (N—C═O), O—C═O, and CO_3.

The wettability measurements are corroborated by XPS. Table 2 gives the O/C ratio, which corresponds to the oxidation degree of the treated surface, the atomic percentage of nitrogen after plasma treatment, and the grafting ratio calculated from the C1s peak. The ratio takes into account contributions of C—O (C—N) at 285.8 eV, C═O (N—C═O) at 287.2 eV, O—C═O at 288.8 eV, and CO_3 at 290.0 eV.

From the results in Table 2, air plasma treated surfaces show pronounced oxidation, which increases with the power. This is accompanied by a significant grafting ratio of polar groups, mainly C—O, C═O, and O—C═O. With nitrogen plasma treatment, the oxidation and the grafting ratio both become less significant. These results are in agreement with the previous characterization by wettability measurements. Plasma activation allows the incorporation of oxygen-containing groups, which results in a surface polarity improvement. These observations also constitute additional clues regarding the differences between air and nitrogen plasma effects.

In order to obtain information about the potential top-surface modifications with air plasma suggested by the results in Fig. 5, the intensity of a shake-up is studied from the C1s spectra. Shake-up peaks result from the effect that the sudden creation of the core hole has on the other electrons in the atom. It usually comes from the excitation of plasmons, discrete outer levels, or electrons in the conduction band in metals. Fig. 7 illustrates a decrease in this shake-up for air-treated PEEK, which indicates an opening of the aromatic rings in the PEEK matrix [31]. Let us remember that all measurements are done with a grazing angle such that the results concern a depth of < 5 nm from the surface. Hence, the degradation involves only the first molecular layers without long-range damages.

Table 3
Comparative summary of the phenomena occurring with air and nitrogen plasma treatment.

	Air plasma	Nitrogen plasma
F_{max} after ageing	↘	↗
Effect of ageing	Bad influence	No influence
Hydrophilic properties (θ_w)	↗ up to 10°	Good, without variation (~25°)
O/C ratio (surface oxidation)	↗ up to 0.46	No variation (~0.3)
Shake-up (aromatic ring integrity)	↘	No variation

The XPS characterizations suggest that air plasma treatment is more aggressive than nitrogen treatment and may lead to higher local temperatures. In their study, Dupuis et al. also observed an increasing surface oxidation on their PEEK substrates activated with similar remote atmospheric pressure plasma [26]. They compared different gas of which air and nitrogen. Even if the tendencies are quite similar, they characterize a greatest degradation of the aromatic rings under nitrogen plasma than under air plasma. It could be arise from the nozzle which present a different shape and treat in a different way (rotary movement in Dupuis's article and linear movement with AcXys equipment).

Table 3 summarizes the phenomena occurring with air and nitrogen plasma treatment. Additional experiments were carried out to see the influence of the plasma treatment on topography modifications.

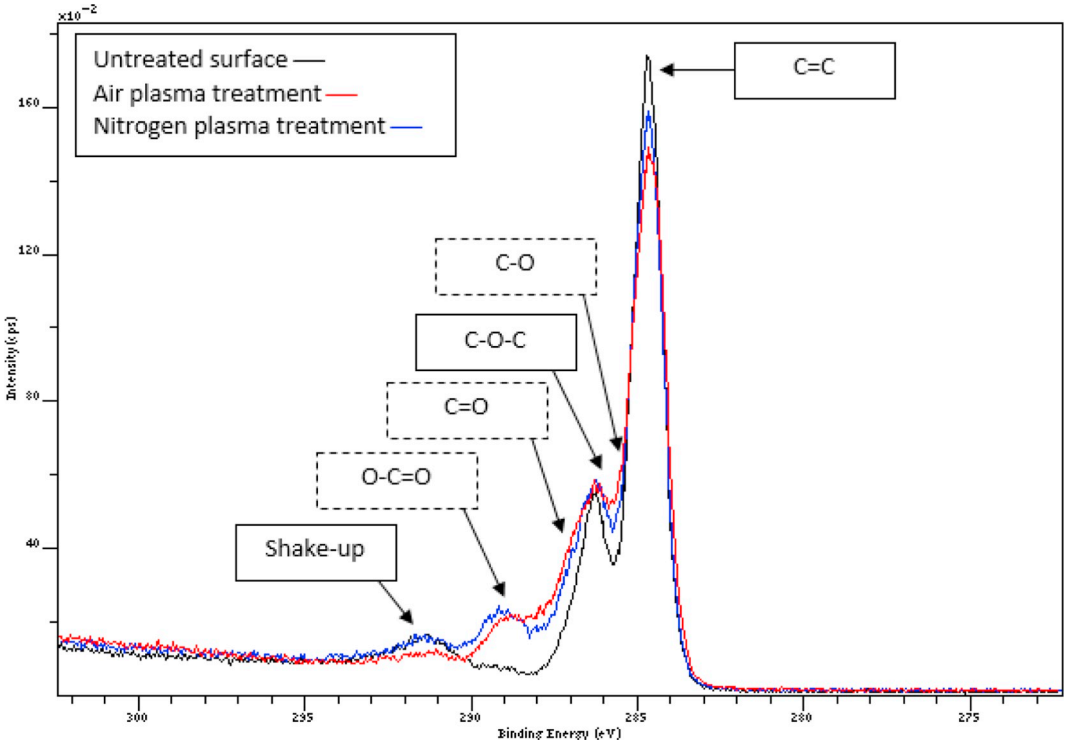


Fig. 7. Superposition of the C1s peak from an untreated substrate, an air plasma treated substrate, and a nitrogen plasma treated substrate. Contributions of C═C, C—O—C, and shake-up components from the PEEK matrix and C—O, C═O, and O—C═O components from grafting are indicated.

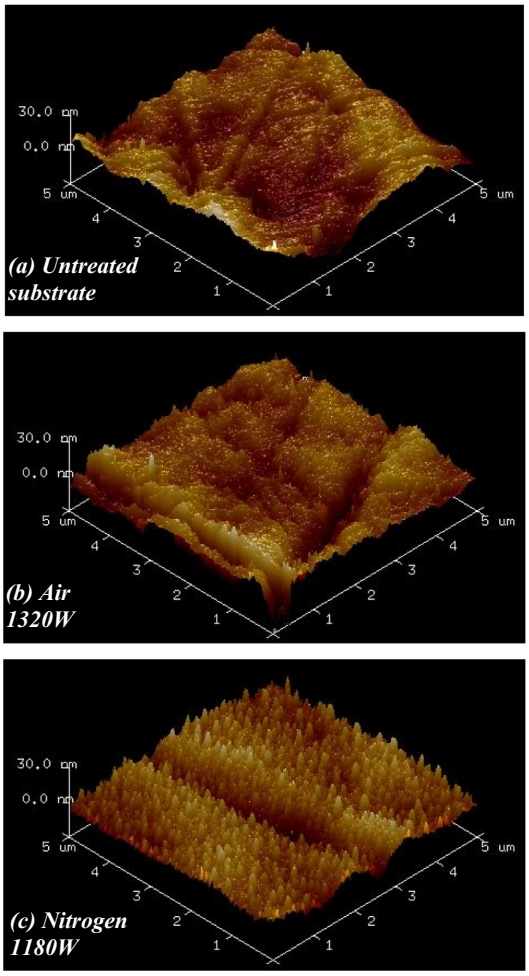


Fig. 8. AFM images (5 µm × 5 µm) of (a) an untreated PEEK substrate, (b) an air plasma treated sample at 1320 W, and (c) a nitrogen plasma treated sample at 1180 W.

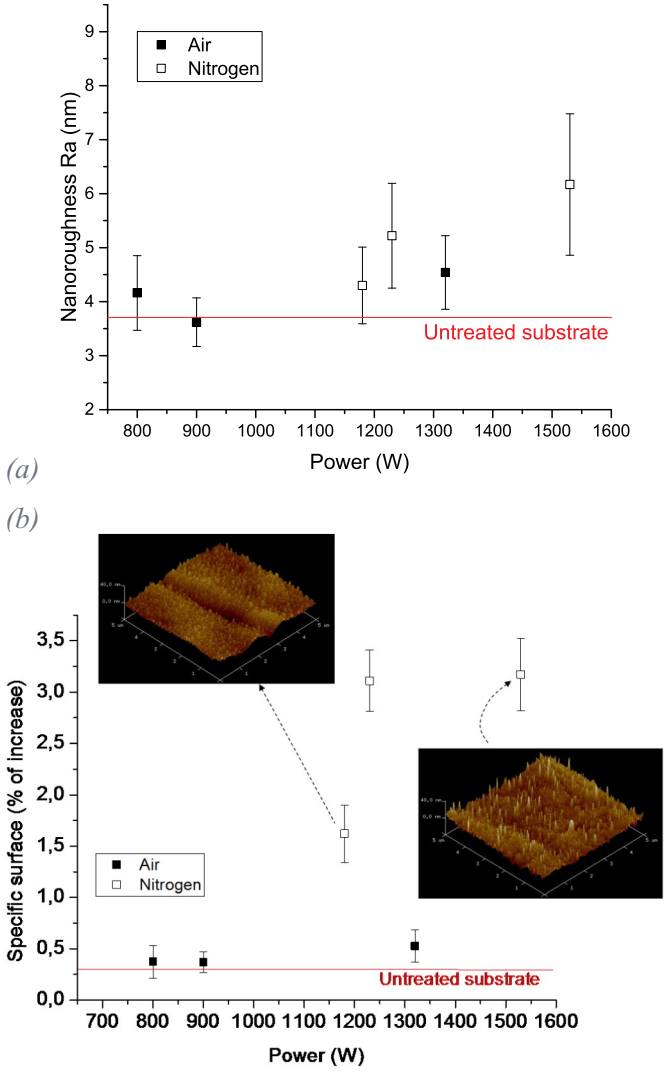


Fig. 9. (a) Nanoroughness and (b) specific surface evolution data obtained by AFM in Peak Force mode, relative to gas and plasma power. Values before plasma activation are represented by the continuous line.

3.3. Typical profiles obtained after plasma activation according to gas plasma

The nanoroughness is characterized by AFM in Peak Force mode. The results for substrates without treatment, after air plasma treatment, and after nitrogen plasma treatment are presented in Fig. 8.

Nitrogen plasma treatment gives rise to a very specific profile, with nanopeaks of around 20–30 nm height, as observed in Fig. 8(c). This configuration, which presents numerous anchors, should favor adhesion [32]. This nanoroughness is not visible in the sample treated with air plasma, the profile of which is very similar to that of an untreated substrate, whatever the discharge power (Fig. 8(b)).

In order to quantify this profile evolution under air and nitrogen plasma, the two parameters described in the Materials and Methods section were measured from the AFM images. Fig. 9(a) and (b) illustrate the variation in R_a and S_{dr} values, respectively, relative to those of an untreated substrate. Although the topography image in Fig. 8(c) presents a typical profile after nitrogen plasma treatment, Fig. 9(a) indicates a slight increase in the nanoroughness [32]. No significant variation is visible with the air plasma treatment, in accordance with the AFM images that is very similar to the reference one. The results support the hypothesis that air plasma treatment provides mostly chemical modifications. If the use of the R_a value does not provide enough evidence to draw conclusions about the nitrogen plasma effect, the developed interfacial area ratio S_{dr}, which corresponds to the specific surface of the samples, does highlight differences between the gases. Indeed, its increase under nitrogen plasma is about 3%, compared to < 0.5% under air plasma. This behavior is directly linked to an increase in anchors per unit area and could explain the very efficient adhesion observed in this study.

Öteyaka et al. [33] also observed somewhat hydrophilic nodules that coalesced together after plasma treatment of a polyethylene terephthalate polymer. They attributed this phenomenon to thermoplastic chain scissions as a result of the energetic species of the plasma. It could be that, in our case, the reactive species from nitrogen post-discharge have a more significant energy than the species from air post-discharge and act like a chemical etching tool. When the plasma torch is quite far from the sample (45 mm), other observations not presented here have shown smooth profiles, in the same way as profiles obtained under air plasma. This can be explained by the fact that nitrogen post-discharge in an air environment induces an increasingly homogeneous mixture further away from the outlet of the nozzle [34]. Fewer nitrogen reactive species are contained in the post-discharge and an ambient air post-discharge is favored.

One way to support this assumption is to measure the diiodomethane contact angle (DCA), which is a value that is well-known to be linked to the quantity of anchors per unit surface area [35]. Fig. 10 represents the DCA values measured after nitrogen plasma activation relative to the S_{dr} values calculated from the AFM images. The

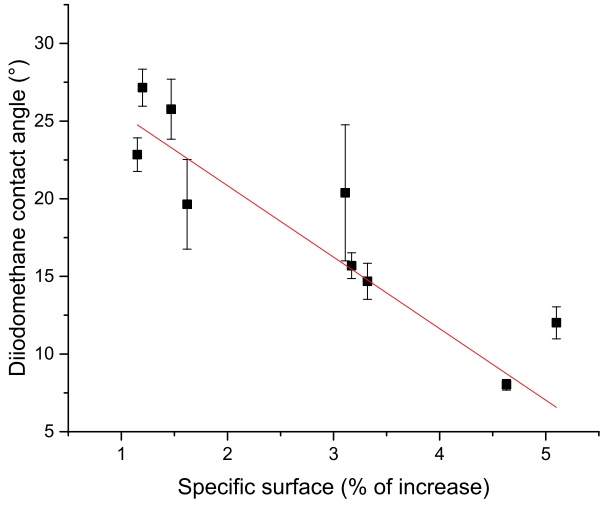


Fig. 10. Relationship between the specific surface (as a percentage of increase relative to an untreated surface) and the diiodomethane contact angle after nitrogen plasma treatment with different power and gaps. $R^2 = 0.90$.

comparison leads to a proportional relationship with an R^2 value equal to 0.9. The increase in specific surface is negatively correlated with the DCA. This indicates a larger anchoring surface, which would improve adhesion phenomena with the future coating by using nitrogen treatment.

4. Conclusion

In this study, various characterization methods were used to identify surface modifications and characterize durable adhesion improvements. The cross-cut test is a widespread industrial test that allows validation, or not, of the adhesion of a sample. Nevertheless, this approach is insufficient to provide a deeper understanding of the adhesion mechanisms happening at the interface. To this end, three-point bending tests were carried out. This complementary technique is finer and gives both quantitative and qualitative data that can be corroborated with the cross-cut test results.

The nature of the plasma gas has an obvious impact on surface modification. Air plasma treatment has been shown to be relatively aggressive, especially for the first molecular layers at high power. It induces surface oxidation. On the other hand, nitrogen plasma treatment leads to a radical surface nanoroughness modification, with the creation of new anchoring points.

By referring to the literature and the different adhesion theories, the following gas-related behaviors were revealed:

- As highlighted by WCA measurements and XPS, air plasma treatment mostly gives rise to physico-chemical and chemical modifications. Hydrophilicity explains the good initial adhesion but the low specific surface could be responsible for ageing degradation.
- AFM images correlated with diiodomethane contact angle measurements underline the capacity of nitrogen plasma treatment to modify the physical properties of the substrate surface. Nevertheless, only a combination of mechanical anchoring and hydrophilicity can explain the durable adhesion.

Finally, this paper is an example of a global approach using complementary techniques. With this approach, it is possible to obtain robust conclusions concerning improvements in adhesion phenomena after plasma treatment.

Acknowledgements

The authors gratefully acknowledge the IRT Saint-Exupery Surfinnov project partners, especially Airbus Helicopters company, for the financial support.

References

[1] C. Soutis, Carbon fiber reinforced plastics in aircraft construction, Mater. Sci. Eng. A 412 (1–2) (2005) 171–176.
[2] M. Sharma, S. Gao, E. Mäder, H. Sharma, L. Yew Wei, J. Bijwe, Carbon fiber surfaces and composite interphases, Compos. Sci. Technol. 102 (2014) 35–50.
[3] A.A. Collyer, High-temperature engineering thermoplastics, A Practical Guide to the Selection of High-Temperature Engineering Thermoplastics, Elsevier, Oxford, England, 1990.
[4] B.R.K. Blackman, A.J. Kinloch, J.F. Watts, The plasma treatment of thermoplastic fibre composites for adhesive bonding, Composites 25 (5) (1994) 332–341.
[5] A. Ganesan, M. Yamada, M. Fukumoto, The effect of CFRP surface treatment on the splat morphology and coating adhesion strength, J. Therm. Spray Technol. 23 (1–2) (2013) 236–244.
[6] L.F.M. DaSilva, A. Öchsner, R.D. Adams (Eds.), Handbook of Adhesion Technology, Spinger-Verlag Berlin Heidelberg, Berlin, 2011.
[7] Règlement n°1907/2006 - Ministère du Travail, de la Solidarité et de la Fonction Publique, REACH: Registration, Evaluation and Authorization of CHemicals, (2007).
[8] A. Baalmann, K.D. Vissing, E. Born, A. Gross, Surface treatment of polyetheretherketone (PEEK) composites by plasma activation, J. Adhes. 46 (1–4) (1994) 57–66.
[9] J. Muñoz, J.A. Bravo, M.D. Calzada, Aluminum metal surface cleaning and activation by atmospheric-pressure remote plasma, Appl. Surf. Sci. 407 (2017) 72–81.
[10] S.J. Hitchcock, N.T. Carroll, M.G. Nicholas, Some effects of substrate roughness on wettability, J. Mater. Sci. 16 (3) (1981) 714–732.
[11] Q. Bénard, M. Fois, M. Grisel, Peel ply surface treatment for composite assemblies: chemistry and morphology effects, Compos. A: Appl. Sci. Manuf. 36 (11) (2005) 1562–1568.
[12] P. B, J. Comyn, L. Mascia, G. Xiao, Plasma-treatment of polyetheretherketone (PEEK) for adhesive bonding, Int. J. Adhes. Adhes. 16 (2) (1996) 97–104.
[13] E. Occhiello, M. Morra, G.L. Guerrini, F. Garbassi, Adhesion properties of plasma-treated carbon/PEEK composites, Composites 23 (3) (1992) 193–200.
[14] UL - SCAN Equipement CLE EN MAIN, AcXys Technologies, (2017) [Online]. Available https://www.acxys.com/fr/products/turnkey-equipments/ul-scan.html , Accessed date: 1 September 2017.
[15] F. Fanelli, F. Fracassi, Atmospheric pressure non-equilibrium plasma jet technology: general features, specificities and applications in surface processing of materials, Surf. Coat. Technol. 322 (2017) 174–201.
[16] A.J. Yáñez-Pacios, J.M. Martín-Martínez, Surface modification and improved adhesion of wood-plastic composites (WPCs) made with different polymers by treatment with atmospheric pressure rotating plasma jet, Int. J. Adhes. Adhes. 77 (2017) 204–213 no. April.
[17] D.K. Owens, R.C. Wendt, Estimation of the surface free energy of polymers, J. Appl. Polym. Sci. 13 (8) (1969) 1741–1747.
[18] C.J. Van Oss, Interfacial Forces in Aqueous Media, 2nd edition, Londres, 2006.
[19] AFNOR, ISO 14679, Adhésifs – Détermination des Caractéristiques D'adhésion Par Une Méthode de Flexion à Trois Points, (1997).
[20] S. Genty, J. Sauvage, P. Tingaut, M. Aufray, Experimental and statistical study of three adherence tests for an epoxy-amine/aluminum alloy system: pull-off, single lap joint and three-point bending tests, Int. J. Adhes. Adhes. 79 (2017) 50–58.
[21] AFNOR EN ISO 2409, Peintures et Vernis - Essai de Quadrillage, (2013).
[22] AFNOR NF EN ISO 2812-2, Peintures et Vernis - Détermination de la Résistance Aux Liquides. Partie 2: Méthode par Immersion Dans l'eau, (2017).
[23] S. Jha, et al., Experimental investigation into the effect of adhesion properties of PEEK modified by atmospheric pressure plasma and low pressure plasma, J. Appl. Polym. Sci. 118 (2010) 173–179.
[24] J.-B. Sauvage, M. Aufray, J.-P. Jeandrau, P. Chalandon, D. Poquillon, M. Nardin, Using the 3-point bending method to study failure initiation in epoxide-aluminum joints, Int. J. Adhes. Adhes. 75 (2017) 181–189.
[25] M. Gigliotti, J.-C. Grandidier, M.C. Lafarie-frenot, Vieillissement de matériaux composites à matrice organique - Cas d'études, Techniques de L'ingénieur, AM5323, 2014.
[26] A. Dupuis, et al., Improving adhesion of powder coating on PEEK composite: influence of atmospheric plasma parameters, Appl. Surf. Sci. 357 (2015) 1196–1204.
[27] H. Schonhorn, L. Sharpe, Thermodynamic adhesion, Chem. Eng. News 41 (15) (1963) 67–88.
[28] S. Buchan, W. Rae, Chemical nature of the rubber to glass bond, Trans. Inst. Rubb. Ind. 20 (1946) 205–216.
[29] J. Mac Bain, D. Hopkins, On adhesives and adhesive action, J. Phys. Chem. 29 (2) (1926) 188–204.
[30] N. Encinas, B. Díaz-Benito, J. Abenojar, M.A. Martínez, Extreme durability of wettability changes on polyolefin surfaces by atmospheric pressure plasma torch, Surf. Coat. Technol. 205 (2010) 396–402.
[31] E. Gonzalez, M.D. Barankin, P.C. Guschl, R.F. Hicks, Ring opening of aromatic

polymers by remote atmospheric-pressure plasma, IEEE Trans. Plasma Sci. 37 (6) (2009) 823–831.
[32] K. Gotoh, Y. Kobayashi, A. Yasukawa, Y. Ishigami, Surface modification of PET films by atmospheric pressure plasma exposure with three reactive gas sources, Colloid Polym. Sci. 290 (11) (2012) 1005–1014.
[33] M.O. Oteyaka, P. Chevallier, S. Turgeon, L. Robitaille, G. Laroche, Low pressure radio frequency ammonia plasma surface modification on poly(ethylene terephthalate) films and fibers: effect of the polymer forming process, Plasma Chem. Plasma Process. 32 (2012) 17–33.
[34] E. Pfender, J. Fincke, R. Spores, Entrainment of cold gas into thermal plasma jets, Plasma Chem. Plasma Process. 11 (4) (1991) 529–543.
[35] C.J. Van Oss, R.J. Good, M.K. Chaudhury, Additive and nonadditive surface tension components and the interpretation of contact angles, Langmuir 4 (4) (1988) 884–891.